Non-linear light scattering in photorefractive LiNbO$_3$ crystals studied by Z-scan technique

Sergey Kostritskii[1] · Michel Aillerie[2,3] · Edvard Kokanyan[4] · Oleg Sevostyanov[5]

Abstract

Experimental study of non-linear scattering (NLS) in nominally pure, Mg- and Zr-doped LiNbO$_3$ crystals with a varying dopant concentration are reported in this paper. The study is undertaken by Z-scan technique with a cw-excitation at 514.5 nm. A modified open-aperture Z-scan experimental setup is used to evaluate the contributions of NLS in the observed transmission attenuation. Study of these open-aperture Z-scan traces shows that NLS has marked magnitude at moderate and high light intensities in undoped, strongly Zr-doped and Mg-doped LiNbO$_3$, and a very significant magnitude in the moderately Zr-doped LiNbO$_3$ crystals even at low intensities. NLS is related to the photoinduced light scattering (PILS), which is explained by holographic amplification of the seed scattering due to photorefractive effect.

1 Introduction

Characterization of non-linear optical materials is a key step to choose the most adequate material for a given non-linear optical process. The value of index of non-linear refraction (NLR) n_2 and non-linear absorption (NLA) β is interesting for high-intensity applications. In the case of some often used non-linear optical materials, like LiNbO$_3$, photorefraction also presents additional non-linear effects, providing a significant extra contribution to NLR and inducing the non-linear scattering (NLS) [1]. The Z-scan technique is a well-established sensitive method to determine these non-linearities of optical materials [2–5]. However, the hard limitations in application of the Z-scan method for the determination of the NLR and NLA in photorefractive (PR) media

should be expected. These limitations are essentially caused by the presence of NLS that can mask the true third-order non-linear response of the PR material, similar to the influence of thermo-optical effect on Z-scan experiments [6]. Even though this problem has been documented before, the widespread use of the Z-scan often leads to results obtained from naively interpreted Z-scan experiments that provide values for the NLR, NLA, and the third-order non-linear susceptibility, which are anomalously high [7–15] and, thus, are simply not trustworthy.

While the influence of PR effect on closed-aperture (CA) Z-scan measurements of NLR was studied experimentally in detail and explained theoretically [1, 10, 12, 16], no explanation of influence of PR effect on the open-aperture (OA) Z-scan experiments is proposed yet. It is caused by the fact, that an OA detector within a standard Z-scan setup was considered [7–17] to be able to collect all light behind a sample under study. However, it is not valid for the case of strong NLS, when a significant part of the scattered light is not falling to the OA detector [18]. The solution of this task has practical importance, as it may allow for application of OA Z-scan methods in PR materials for evaluation of actual values of NLA and the third-order non-linear susceptibility, as well as for quantitative study of PR effect. This paper is devoted to the detailed experimental and theoretical study of PR effect contribution in integral non-linear response evaluated by Z-scan, here applied in the characterization of lithium niobate, pure and doped by Zr and Mg ions.

✉ Sergey Kostritskii
skostritskii@optolink.ru

1 RPC Optolink, Sosnovaya al. 6A, Zelenograd 124489, Moscow, Russia

2 Laboratoire Matériaux Optiques, Photonique Et Systèmes, LMOPS, Université de Lorraine, 57070 Metz, France

3 Laboratoire Matériaux Optiques, Photonique Et Systèmes, LMOPS, CentraleSupelec Université Paris-Saclay, 57070 Metz, France

4 Institute for Physical Research, National Academy of Sciences of Armenia, 378410 Ashtarak, Armenia

5 Physics Department, Kemerovo State University, 650043 Kemerovo, Russia

2 Experimental techniques and samples

2.1 Modified open-aperture Z-scan technique

It has been established [18] that quantitative information about NLA and NLS may be obtained by the OA Z-scan experiments with a modified setup. The experimental arrangement corresponding to the modified OA Z-scan technique is represented in Fig. 1. Similar to the standard single-detector OA Z-scan method [2–5], the transmitted beam is collected with an open-aperture detector D1 at far field to reduce the scattered light falling on this detector. The detector D1 consists of lens with small aperture of 20 mm before a photodiode, that allows to avoid completely the influence of NLR caused by thermal and PR non-linearities, on an OA Z-scan trace detected [1, 6, 10]. This approach allows to avoid the effects of linear sample inhomogeneities providing linear scattering losses, and gives information about NLA. However, Z-scan data obtained with detector D1 will account for the extra non-linear scattering losses in PR media in addition to the expected NLA losses.

Detector D3 introduced immediately after the sample collects with the aid of lens L2 all transmitted light that includes scattered light. Detector D3 should, therefore, see only the losses due to linear and non-linear absorption of the sample. However, in some particular cases of the strong NLS, small part of scattered light may be not collected by detector D3, if numerical aperture of lens L2 is smaller than an angle of NLS. In these cases, NLS is still able to mask the NLA caused by third-order non-linearity. The scattering at a small forward scattering angle is collected using the detector D2. Thus, this detector will account some part of total scattering, including linear and non-linear scattering [18, 19].

The samples were scanned in the vicinity of the L1 lens focus ($z = 0$) starting from a position ahead of focus ($-z$) and moving toward a position behind the focus ($+z$). The scanning range was about ± 30 mm in all the experiments.

The data were collected at every 0.2 mm on the lens axis, by translating the sample under test through the focal point using a computer-controlled stepper motor. High-speed silicon detectors (DET1100, rise time is 20 ns) were used for D1, D2, and D3. Signals from these detectors were processed by a digital oscilloscope InfiniiVision 2002A (integration time used was 0.2 s for single measurement). A Z-scan curve was plotted by averaging over 11 single measurement points. No any pronounced temporal change of an output signal was observed at the intensity level used by us for Z-scan experiments. Note, that this finding is in accordance with data on intensity dependence of PR-response kinetics in undoped and doped LN crystals [10, 17, 20–23]. An argon-ion laser Spectra Physics model 2550 (Stabilite 2017) operating at 514.5 nm was focused with the 200 mm focal length L1 lens into a sample studied. This adjustable argon-ion laser generates a Gaussian light beam with an output power ranging from 0.5 to 143 mW, corresponding to a light intensity I_0 at the focal point of the setup (i.e., at $z = 0$) in the range from 9 W/cm^2 to 2.5 kW/cm^2. The thickness of samples was chosen in such a way that it was smaller than the Rayleigh range z_R of the focusing lens. The beam diameter is $W_0 = 4f \lambda / \pi W_1$ at the focal point ($z = 0$) in air [5], where f is the focal length of lens and W_1 is the beam diameter at the aperture, i.e., $W_0 = 85$ μm at $\lambda = 514.5$ nm.

For qualitative investigation of NLS at the high light intensities, including speckle pattern, we used visual observation of forward-scattered light on screen placed behind the crystal in far-field. The cw-radiation of a DPSS laser "Tekhnoscan Mozart-5s" with $\lambda = 532$ nm was focused with the same L1 lens into a LiNbO$_3$ crystal. The output laser power was gradually varied within the range from 0.2 to 3.5 W that allows for the rough comparative study of threshold levels for moving speckle generation in the differently doped and undoped LiNbO$_3$.

Fig. 1 Schematic diagram of the modified open-aperture Z-scan setup. AIL—Ar-ion laser, A—aperture, P—polarizer, S—sample, F1, F2—neutral density filters, D1, D2, D3—detectors (D1 consists of a photodiode and lens with small aperture of 20 mm), BS—beam splitter, L1, L2—lenses
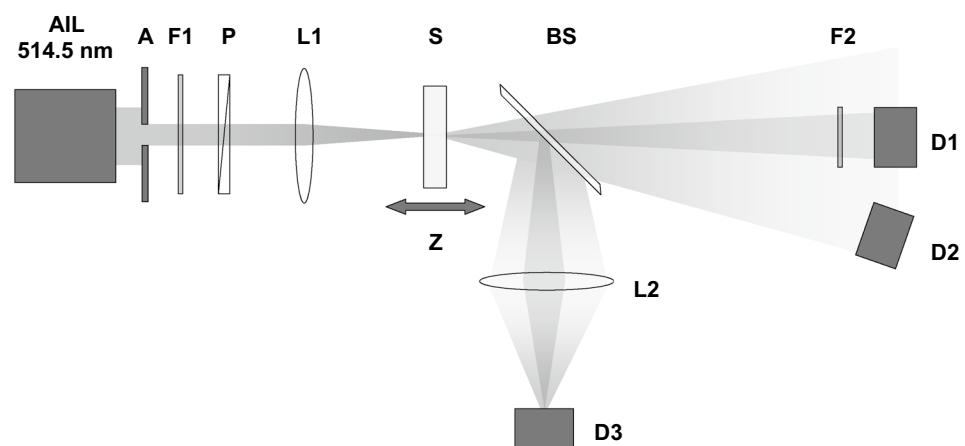
2.2 Sample fabrication and characterization

The PR effect is disadvantageous in many fields of optics, since, for device applications, long-term stability of the beam is required. We carried out the experimental study of nominally pure, Mg- and Zr-doped congruent LiNbO$_3$ crystals. These dopants have practical significance, since it can change the magnitude and build-up time of PR effect within the very wide ranges [16, 20–23]. However, there are significant contradictions between the data reported for the general dependence of PR effect on dopant concentration [7, 16, 20–23].

Based on the Czochralski technique, a growth setup using a single platinum crucible with rf heating element in air atmosphere was used to grow a set of Zr-doped lithium niobate crystals. To obtain directly during the growth process single-domain crystals, a dc electric current with a density of about 12 A/m^2 was passed through the crystal-melt system. The starting materials used for sintering the lithium niobate charges of congruent composition were high-purity Nb$_2$O$_5$ and LiCO$_3$ compounds from Johnson-Matthey and Merck. ZrO$_2$ was introduced into the melt with concentration equals to 0.625, 0.75, 0.875, 1.00, 1.25, 1.50, 2.00, and 2.50 mol%, respectively.

The several nominally pure congruent LiNbO$_3$ samples were grown from a similarly prepared melt, but without the addition of ZrO$_2$ compound. The latter samples were used to obtain the reference data in our study of Zr-doping effect. All samples were optical-grade polished with surfaces perpendicular to the corresponding crystallographic axes.

Besides these experimental samples grown by us, several commercially available samples of thin (1 mm) z-cut wafers have been also investigated: (1) nominally pure congruent LiNbO$_3$ crystals (2) Mg-doped ([Mg]=5 mol% according to supplier specification) congruent LiNbO$_3$ crystals. The suppliers were Gooch & Housego (G&H) and Yamaju Ceramics Co (YCC). Measurements of the IR absorption spectra within the range of stretching vibration of OH bonds demonstrate the significant difference between the two kinds of Mg-doped LiNbO$_3$, Fig. 2. The OH absorption peak location is a good indicator of the photorefractive damage resistance. Crystal with a fully shifted OH absorption peak is "above PR damage threshold" (i.e., it is more resistant to PR damage [24]) and, thus, expected to show a much smaller NLS in comparison with a MgO-doped crystal with unshifted or slightly shifted OH band.

Although it is common to state only the MgO concentration for a photorefractive resistant crystal, it has been established [23, 24] that even a small variation of the Li/Nb ratio (i.e., molar fraction of Li$_2$O) can change an actual value of the threshold MgO concentration. According to the suppliers' specifications [25, 26] the Li$_2$O molar fraction is 48.38 and 48.5 mol% for Mg:LiNbO$_3$ crystals from
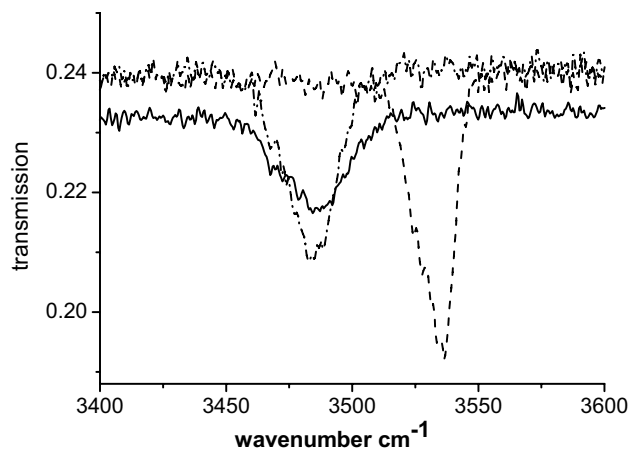

Fig. 2 IR-absorption spectra of Mg-doped congruent LiNbO$_3$ with [Mg]=5.0 mol%: for a crystal supplied by G&H (3″-wafer denoted by Crystal Technology Inc as MgOLN-10–05) is shown by dash-dotted curve; for a crystal supplied by YCC (MgOLN-05–14) is shown by dashed curve. The spectrum of a nominally pure congruent crystal supplied by YCC (NOZe39X223, LN Z OPT) is shown by solid curve

G&H (fabricated by CTI Inc. in 2005) and YCC companies, respectively. According to the finding reported previously [24], our IR spectroscopy data (Fig. 2) demonstrate that the studied samples supplied by G&H are slightly below PR damage threshold, in contrast to the samples from YCC.

3 Experimental results

Within the standard approximation [2–5] the response of a sample in the OA Z-scan experiments is regarded to be insensitive to the self-defocusing and self-focusing effects induced by third-order non-linearity [2–5], thermal [27, 28], and PR [1, 27] lensing effects. Therefore, the standard OA Z-scan technique, which is using only the one near-field detector D1 (Fig. 1), was applied as the first approach to evaluate the NLS in the nominally pure LiNbO$_3$ crystals from our measurements with the cw-laser beams. The position-dependent change in the normalized transmittance $\Delta T(z)$ can be expressed by [3, 5]:

$$\Delta T(z) = T(z) - 1 = -q_0/(2\sqrt{2}), \tag{1}$$

where

$$q_0 = \Delta\alpha d_{\text{eff}}/\left(1 + z^2/z_R^2\right) \tag{2}$$

$\Delta\alpha$ is light-induced change in the attenuation coefficient, z the actual sample position relative to the focus, z_R the Rayleigh range, $d_{\text{eff}}=[1 - \exp(-\alpha_0 d)]/\alpha_0$ the effective thickness of the sample, α_0 the linear absorption coefficient, and d is the thickness of sample.

It has been established [2–5] that the depth of transmission valley in Z-scan trace at $z = 0$ (or equivalently the largest change in the normalized transmittance, $\Delta T((0))$ is not directly proportional to q_0, when $q_0 \geq 0.3$. As a consequence, for transmittance changes $\Delta T(0) \geq 0.11$ (i.e., for $T(z = 0) \leq 0.89$), the data analysis of experimental Z-scan traces needs to be based on the more general equation [4]:

$$\Delta T(z) = 1 - \ln(1 + q_0)/q_0, \text{ i.e.}$$
$$T(z) = \ln(1 + q_0)/q_0. \tag{3}$$

The observed changes of the attenuation coefficient $\Delta\alpha$ include the intensity-dependent contribution of NLS in addition to NLA contribution, i.e.,

$$\Delta\alpha = \beta I_0 + a_{nls}, \tag{4}$$

where β is the true NLA coefficient related to the two-photon absorption (TPA) cross section, α_{nls} the NLS coefficient, and I_0 is the light intensity at a focus (i.e., at $z = 0$).

The PR effect in lithium niobate crystals induces the strong scattering, which is manifesting itself as NLS in Z-scan experiments [1, 7], if these crystals are exposed to a cw-laser coherent radiation. It means that all values of β^* evaluated by standard approximation ($\beta^* = \Delta\alpha/I_0$) in the many previous works [7–15, 17] represent some false (overestimated) values of non-linear absorption coefficient. Therefore, we introduce the other right term for this product: the non-linear attenuation coefficient $\eta(I_0) = \Delta\alpha/I_0$ (and $\eta >> |\beta|$), which has a complex dependence on light intensity I_0.

Note, there is the uncertainty of the intensity I_0 of the laser beams used in the Z-scan experiments. It is caused by the fact that the minimum beam width W_{min} inside a crystal increases with increasing power compared to the minimum beam waist W_0 in air [8]. It has been established also that W_{min} increases with input power P_{in} in full agreement [8] with the change of non-linear refraction n_2. The principal parameters (wavelength λ, focal distance of lenses f, laser type and, thus, width (aperture) W_1 of beam at laser output) in our Z-scan experiments and study reported in Ref. [8] coincide. Therefore, we have used data from Ref. [8] on dependence of W_{min} on P_{in} for the estimation of an actual value of light intensity I_0 at quantitative evaluation of the NLS in undoped congruent LiNbO$_3$ crystals.

Our experimental data on transmittance modulation $T(z)$ within open-aperture Z-scan trace measured with the D1 detector (Fig. 3) in nominally pure congruent LiNbO$_3$ at 514.5-nm cw-excitation yield the η value of 5.35 cm/kW, Table 1. This value is found to be in quite satisfactory agreement with the wide range of the previously reported values of β^*, which were evaluated by the standard approximation with cw-laser beams for the undoped as-grown lithium niobate crystals. For example, values equal to 0.39 [17],
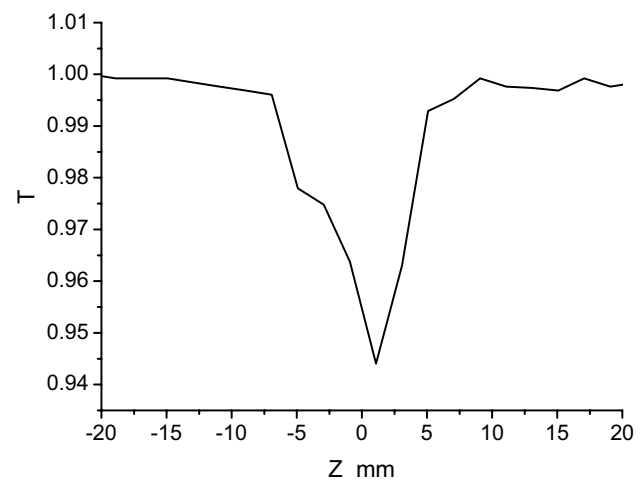

Fig. 3 Open-aperture Z-scan trace measured by detector D1 (Fig. 1) for undoped congruent LiNbO$_3$ crystal at input power $P_{in} = 2$ mW. The transmittance $T(z)$ is normalized to transmittance in the linear region at $|z| \geq 25$ mm

Table 1 Non-linear scattering coefficient α_{nls} and the non-linear attenuation coefficient η determined at different input powers P_{in} for undoped congruent (cLN), Zr-doped congruent (Zr:cLN), and Mg-doped congruent (cMg:LN, [Mg] = 5 mol%) LiNbO$_3$ crystals

Crystal	cLN YCC	Zr:cLN 2.0 mol%	Zr:cLN 2.5 mol%	Mg:cLN G&H	Mg:cLN YCC
α_{nls}, cm^{-1} at 2 mW	0.16	0	0	0	0
α_{nls}, cm^{-1} at 100 mW	6.32	2.25	1.15	1.86	0.85
η, cm/kW	5.35	1.38	0.46	1.11	0.34

The values of η is determined from the experimental data on Z-scan obtained at $P_{in} = 100$ mW

0.45 [7], 5.0 [8], and 6.8 [10] cm/kW were reported for cw-excitation with $\lambda = 514.5$ nm, but values about 2.7 cm/kW were reported for cw-excitation with $\lambda = 532$ nm [11]. Thus, these values are related to the magnitudes of η, but not to TPA as was reported previously [7–15, 17]. It is important to note that the introduction of large amount of defects (by iron doping [14] and chemical reduction annealing [12]) or application of specific lens [15], or shorter-wavelength laser irradiation [9] provide negative values of η within the wide range from − 33 to − 3 cm/kW.

The very wide range of η values reported [7–15, 17] for LiNbO$_3$ crystals at cw-excitation can be attributed to the significant dependence of the PR effect on specific excitation conditions [27, 28] and many uncontrollable crystal parameters. The latter dependence is the inherent factor for undoped as-grown crystals [7, 12, 29, 30]. Besides, PR effect can be controlled (strongly suppressed) by introducing certain dopants (e.g., Mg, Zr) [10, 16, 20–24]. For example, our OA

Z-scan experiments with the Mg-doped ([Mg] = 5.0 mol%) and strongly Zr-doped (when [Zr] is equal or above photorefractive damage threshold [20, 21]: $[Zr]_{thr} \approx 2.0$ mol%) congruent LiNbO₃ crystals (Fig. 4) gave smaller values of η in comparison with undoped congruent crystals (Table 1). These experimental results indeed confirm our conclusion on photorefractive origin of the marked variation of η values in LiNbO₃ crystals at cw-illumination. This conclusion is also supported by the fact that in the as-grown Mg-doped stoichiometric LiNbO₃, with a Mg concentration about 5 mol%, where PR effect is suppressed by three orders of magnitude, the η values are lower by three orders of magnitude at similar experimental conditions (sample thickness and cw-laser wavelength) [10].

The PR effect in the crystal is largely suppressed under picosecond laser radiation and the third-order non-linearity contribution to the NLA coefficient becomes to be dominating. The picosecond laser pulses are too short for the marked PR process to be observed, if the interval between the pulses is far greater than the PR relaxation time. According to the data on the dynamics of PR effect [31] in LiNbO₃ crystals, in the laser irradiance range of a typical Z-scan experiment, the PR effect takes at least 1 µs to manifest itself and takes 10 ms to relax. Thus, the magnitude of β for NLA induced by ps-pulses is about seven orders of magnitude lower than at cw-illumination. The values of β were reported to be 1.6×10^{-7} cm/kW [31], 2.5×10^{-7} cm/kW [32], and
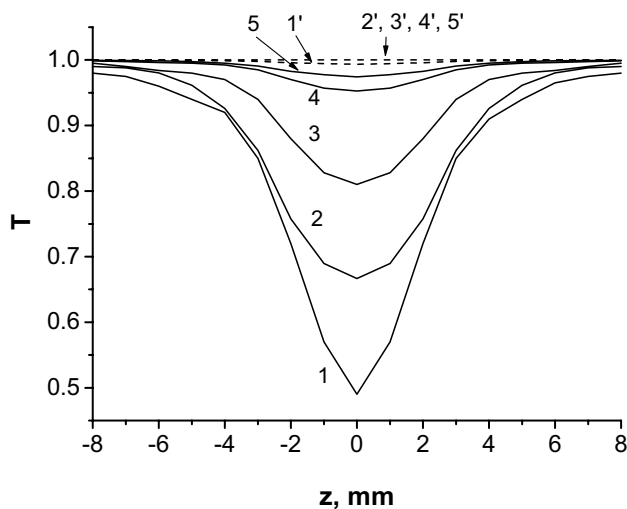

Fig. 4 The experimental open-aperture Z-scan traces measured by detectors D1 and D3 (solid and dashed curves, respectively) in different LiNbO₃ crystals: 1 and 1′—Zr-doped with [Zr] = 1.0 mol%, 2 and 2′—Zr-doped with [Zr] = 0.88 mol%, 3 and 3′—Zr-doped with [Zr] = 0.625 mol%, 4 and 4′ - nominally pure LN, 5 and 5′ - Zr-doped with [Zr] = 2.0 mol%. Measurements were performed at P_{in} = 0.5 mW in cases (1–3), at P_{in} = 2 mW in case (4), and at P_{in} = 25 mW in case (5). The both Z-scan traces measured by D1 and D3 at P_{in} = 25 mW for the Mg-doped LiNbO₃ crystals supplied by G&H and YCC coincide with the traces 2′, 3′, 4′, and 5′

3.8×10^{-7} cm/kW [3], at the 532 nm wavelength that is practically the same as in our experiments. This β value is in rather good agreement with the coefficient of 9×10^{-7} cm/kW that has been theoretically derived for the two-photon absorption process [32]. However, the OA Z-scan experiments with ns-pulses (6 ns) give [33] much larger values in the range of 2.7–2.8×10^{-5} cm/kW. It demonstrates that the Z-scan data reported previously [7–16] for cw-excitation are related to the magnitudes of η and, hence, α_{nls} for NLS, but not to the magnitudes of β for TPA in LiNbO₃ crystals. According to the fundamental findings [1, 3, 5], β does not depend on the pump conditions (cw- or pulse-excitation with various pulse duration), excluding fs-pulses regime due to the peculiarity of polaron excitation in LiNbO₃ [34]. Thus, the large difference for magnitudes of $\Delta\alpha/I_0$ ratio observed between ns- and ps-excitations [30–33] allows for assumption that the PR effect occurs even at ns-excitation.

To account for the NLS contribution to the total attenuation coefficient, we have used simple empirical approach and introduced the NLS coefficient α_{nls} as derived previously [16, 18]:

$$\mathrm{d}I/\mathrm{d}z = -aI - bI^2, a = a_0 + a_s, a_s = g_s[\Delta n]^2,$$
$$\Delta n = \Delta n_l + \Delta n_{nl}, a_s = a_{ls} + a_{nls}, \quad (5)$$

where α is the effective attenuation (extinction) coefficient, α_0 the linear absorption coefficient, g_s the parameter independent on intensity but dependent on wavelength of light, Δn the micro-scale inhomogeneity in the effective refractive index of both linear and non-linear components, Δn_l the spatial intensity independent (linear) inhomogeneity in the refractive index, and Δn_{nl} is the inhomogeneity of light-induced changes in the effective refractive index, that is increasing with light intensity and responsible for NLS. Thus, α_{ls} and α_{nls} are linear scattering and NLS coefficients, respectively. Note, that the linear absorption coefficient α_0 is very small in any crystal studied (≤ 0.03 cm⁻¹) at the excitation wavelength of 514.5 nm. Thus, in our analysis, we have neglected the contribution of the linear absorption.

The values of $\Delta\alpha$ were evaluated from transmittance modulation $\Delta T(z)$ within an OA Z-scan trace with the aid of Eqs. (2) and (3). The values of $\Delta\alpha$ obtained for the undoped and Mg-doped samples at different values of I_0 are given in Table 1. The anomalously large values of β^* evaluated by $\beta^* = \Delta\alpha/I_0$ [7–15] and the small values of β reported previously for ps- and ns-pulsed laser excitation [3, 30–33] demonstrate that NLS contribution dominates over NLA contribution in transmission modulation for OA Z-scan experiments with cw-laser beams in LiNbO₃ crystals. It means that $\Delta\alpha \approx \alpha_{nls} >> \beta I_0$ (see Eq. (4)), and the sharp dependence $\Delta\alpha$ of on I (i.e. on P_{in} at low-power cw-laser excitation) is caused by the increase of the photorefractive NLS with I_0, i.e., by $\alpha_{nls}(P_{in})$ dependence, Fig. 5.
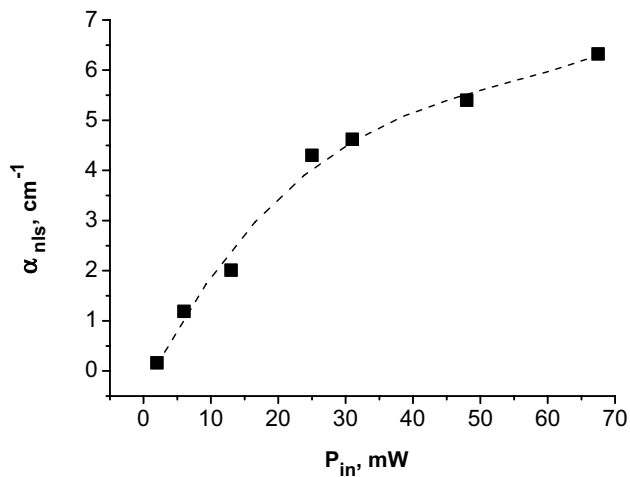
Fig. 5 Dependence of non-linear scattering coefficient $\alpha_{nls} = \Delta\alpha$ on input power P_{in} in nominally pure LiNbO$_3$ crystal

This conclusion is verified also by comparison of the data obtained with the detectors D1 and D3, Figs. 1 and 4. The significant magnitude of this NLS can be seen as an enhanced depletion in the transmitted beam (i.e., sharp decrease of T) collected by detector D1 in comparison with the beam collected by the detector D3 that is shown in the Z-scan curves given in Fig. 4.

Note that for Z-scan traces recorded with detector D3, $\Delta T = 0$ at $P_{in} \leq 100$ W in undoped LiNbO$_3$ and at any input power used in our OA Z-scan experiments (P_{in}(max) = 143 mW) in the Mg-doped and heavily Zr-doped (i.e., with the largest [Zr] = 2.0 and 2.5 mol%) LiNbO$_3$ crystals. It is the consequence of the evident fact that the Mg-doped and strongly Zr-doped crystals show a significantly smaller NLS in comparison with undoped crystals, Table 1. Note that the Mg-doped crystals supplied by YCC have the significantly smaller values of α_{NLS} at the moderate P_{in} in comparison with the Mg-doped crystals supplied by G&H, Table 1. It has been established that the Zr doping of the LiNbO$_3$ crystal can strongly increase the NLS in the moderately Zr-doped LiNbO$_3$ ($0.625 \leq$ [Zr] ≤ 1.5 mol%), Fig. 4. Analysis of difference between Z-scan curves measured with detectors D1 and D3 allows for evaluation of NLS in the Zr-doped LiNbO$_3$ crystals. For detector D1: $\Delta\alpha = \alpha_{nls} + \beta I$, where β is the true NLA coefficient and α_{nls} is the NLS coefficient, for detector D3: $\Delta\alpha = \beta I$. Some part of this scattering is detected also by detector D2, Fig. 6.

We have collected the light scattered at a small forward scattering angle with respect to the beam propagation direction using detector D2 (Fig. 1). The NLS shows the pronounced dependence on the crystal position z, i.e., on a light intensity I, evidencing PR origin of NLS in LiNbO$_3$ crystals. Only in case, when z is close to focal point of lens L1, PR effect has a magnitude sufficient to induce a strong NLS.
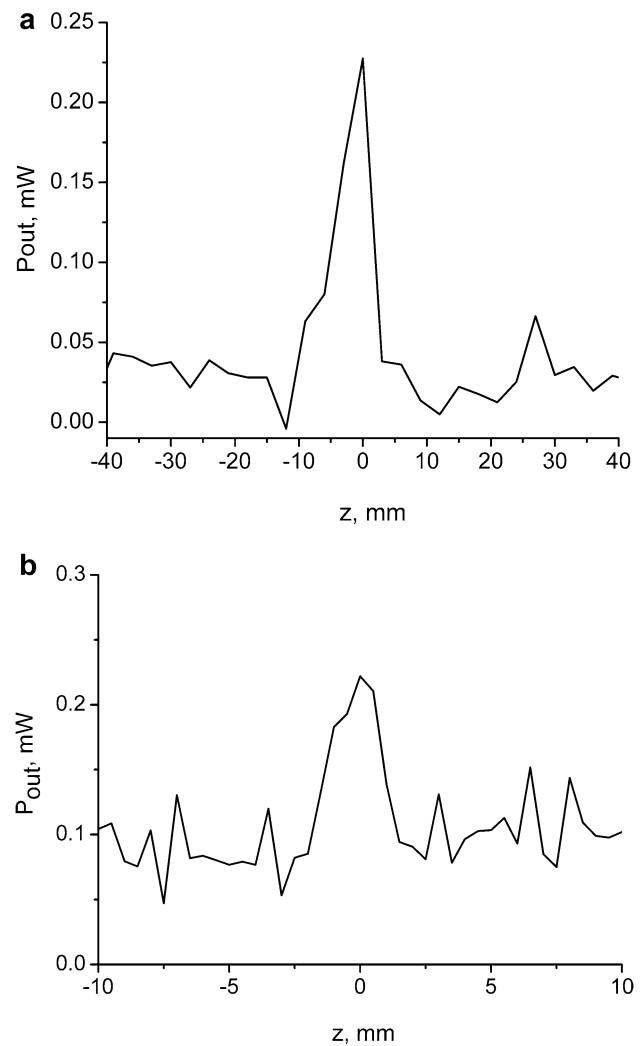

Fig. 6 Z-scan trace of small angle forward NLS measured by detector D2 for Zr-doped congruent LiNbO$_3$ crystals with (**a**) [Zr] = 1.0 mol% at $P_{in} = 25$ mW, and (**b**) [Zr] = 1.5 mol% at $P_{in} = 50$ mW

In the cases of very strong NLS, occurring in the moderately Zr-doped crystals (when $\Delta T \geq 0.3$), Eqs. (2) and (3) are allowing only for rough estimation [3–5] of $\Delta\alpha$ and, hence, α_{nls}. The estimated values of NLS coefficient α_{NLS} have been found to be non-monotonously dependent on Zr concentration with maximum values of α_{NLS} at the intermediate doping level of $0.88 \leq$ [Zr] ≤ 1.0 mol%, Table 2 Because of the approximate estimation of α_{nls} values and uncertainty of the intensity I_0 (we have no data about dependence of W_{min} on P_{in} in Zr-doped crystals), a very rough estimation of η values is possible, only. At the same time, the strongly Zr-doped crystals (([Zr] are 2.0 and 2.5 mol%) have a much low level of NLS as compared with moderately Zr-doped and undoped crystals. According to our results, the weak Zr doping (≈ 0.625–1.25 mol%) could be a good advice to improve the photorefractive sensitivity of congruent lithium

Table 2 The values of NLS parameters estimated roughly by Eqs. (3) and (4) from the OA Z-scan data for the moderately Zr-doped congruent LiNbO$_3$ crystals at $P_{in} = 2$ mW

[Zr], mol %	0.625	0.75	0.88	1.0	1.25	1.5
T_{min}	0.71	0.55	0.3	0.16	0.44	0.60
α_{nls}, cm^{-1}	2.25	4.95	17.47	46.10	7.82	3.80
η, cm/kW	14.67	29.47	81.87	184.36	44.66	24.08
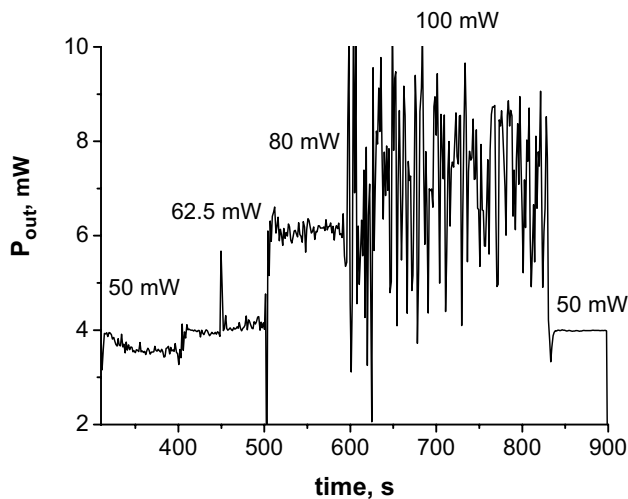
Fig. 7 Temporal dependence of self-pulsing phenomenon for forward-scattered laser beam measured by the detector D1 in Zr-doped LiNbO$_3$ ([Zr] = 1.0 mol%) for the various input powers at fixed crystal position ($z = +5$ mm, i.e., crystal is shifted in right direction from focal point $z = 0$, see Fig. 1). Laser beam with extraordinary polarization propagates along crystallographic Y-axis of sample

niobate for some applications, similar to the case of slightly In-doped (≤ 0.6 mol%) crystals [35]. Note that the both dopants have been established to be the optical damage-resistant impurities at the much higher doping levels in the congruent LiNbO$_3$ crystals [7, 20, 21, 35].

If a Y-cut crystal with appropriate [Zr] ($0.625 \leq$ [Zr] ≤ 1.25 mol%) is placed in a fixed position z near focal point of the lens L1 (Fig. 1), and it is illuminated by a focused extraordinary polarized laser beam, the output power transmitted through the crystal begins to oscillate at a moderate input power ($20 \leq P_{in} \leq 80$ mW, but an actual power level depends on [Zr] and z). A typical plot of this self-pulsing phenomenon reported in Fig. 7 for the moderately Zr-doped LiNbO$_3$ shows a noisy quasi-periodic time dependence. Both the amplitude and period of the transmitted power oscillations depend on input power. The specific period of these oscillations is typically of the order of seconds. The self-pulsation is observed also in undoped LiNbO$_3$, but at much higher powers. Thus, the threshold level of input power from which we observe oscillation of output signal is about 1.5 W, that in $18 \div 75$ times higher than

in Zr-doped LiNbO$_3$, depending on [Zr]. It is important to note that in our stronger Zr-doped ([Zr] ≥ 2.0 mol%) samples, the temporal evolution of NLS is different from what was observed in the moderately Zr-doped samples. Thus, the output power is static at steady state (no any oscillations) in the samples having [Zr] ≥ 2.0 mol%, similar to Mg-doped crystals studied, even at the largest input power level (3.5 W) used by us.

The obvious light-induced speckle pattern is observed simultaneously with appearance of these oscillations. We observed that forward-scattered patterns usually exhibited temporarily fluctuating tiny speckles. Morphology of such speckle patterns changed as a function of the position z between the focal point and the sample. After initial very fast conical defocusing, the pattern continues to evolve in time into a picture of random moving speckles even in a steady-state, where no any large-scale structures can be resolved.

The pronounced moving speckle pattern is observed at $-6 \leq z \leq 29$ mm with the laser beam power above some threshold value depending on [Zr]. When the crystal was located at a distance that is much far from the focal point of the lens L1 ($-8 \geq z \geq 32$ mm), the temporally fluctuating speckle-like light scattering does not occur. In this case, the incident beam was defocused during the initial illuminating time. At these crystal positions, the scattered light intensity became weaker, the scattering cone angle was reduced, and the speckle pattern became static and less pronounced. This phenomenon is seemingly similar to the previously reported observation [1, 36], that forward-scattered speckle patterns were dependent on the spot size of a laser beam (controlled by variation of shift from focal point) in PR LiNbO$_3$:Fe crystals.

4 Discussion

These experimental results unambiguously prove that holographic light scattering is reflected in a Z-scan trace through a decrease in the transmittance near the focal point. The related decrease in the transmittance can be understood, if we recall the geometric setup that was used when we recorded the Z-scan trace: the apex angle in which transmitted probe light can be detected is given by the distance between the LiNbO$_3$ crystal and the photodetector, and the

effective size of the detector area. In our setup, the transmitted light of the probe beam can be detected by D1 (see Fig. 1) within an apex angle of $\pm 2.9°$, whereas the holographically scattered light appears within a cone [37, 38] of $\geq 16°$. This means that some part of the probe beam propagates into directions outside the detection area. Thus, the decrease in the transmittance is due to diffraction from parasitic holograms. Holographic light scattering appears if photorefractive media are exposed to coherent light [37, 38]. It emerges from initial scattering of the incident beam by inhomogeneities within the crystal. Through the photorefractive effect, incident and scattered waves record a multitude of holographic gratings at which the pump beam is subsequently diffracted. If the originally scattered wave and the diffracted pump beam are in phase, the scattering increases continuously by amplification.

The photoinduced light scattering (PILS) is observed in a multitude of PR materials: illumination with a focused laser beam leads to the build-up of scattered light into a wide apex angle around the directly transmitted laser beam. Hereby, the pump beam intensity is decreased, which can be as effective as 99% with respect to the incoming laser light power, i.e., the incoming pump beam is nearly completely scattered. Two characteristic properties of this scattering process have to be emphasized: (1) The build-up of the scattered light is comparable to the temporal behavior known from the recording of holographic gratings in such materials, and (2) PILS is observed with coherent light, only [37–39]. Therefore, the elementary process can be understood in the frame of the interference of the pump beam with initial scattered waves: if a coherent laser beam propagates through a PR crystal, it is scattered at inhomogeneities, such as striations, defects or imperfections.

The theoretical and experimental findings obtained previously for PILS [38, 39] can be used to describe transmission attenuation caused by NLS at OA Z-scan measurements:

$$T_{\min} = \left(1 + m_0\right)/(1 + m_0 \exp(\Gamma l_{eff})) \tag{6}$$

$T_{\min}$ is a minimum value of the transmittance $T(z)$ observed at $z = 0$ normalized to T at $|z| \geq 25$ mm within a same Z-scan trace, Γ the gain coefficient for holographic amplification of the scattered waves, l_{eff} the effective coupling length, i.e., it is the distance between the points where the scattering component emerges from the scattering center and leaves the illuminated area, and m_0 is the seed scattering ratio [38, 39]. According to Ref. [39], l_{eff} can be calculated as

$$l_{eff} = d/\cos\Theta_s^{in} \text{ for } \Theta_s^{in} < \arctan(\omega_0/2d),$$

$$l_{eff} = w_0/\left(2\sin\Theta_s^{in}\right) \text{ for } \quad \Theta_s^{in} \geq \arctan(\omega_0/2d), \tag{7}$$

where d is the crystal thickness and ω_0 is the pump beam waist width near the focal point. A decrease in l_{eff} with increasing angle means that scattering components propagating at angles $\Theta_s^{in} \geq \arctan(\omega_0/2d)$ leave the illuminated area that is already in the crystal volume. The larger the scattering angle is, the smaller the effective interaction length is.

The gain coefficient Γ describing the efficiency of the direct coupling between the pump and scattered waves is [37–39]:

$$\Gamma = 4\pi\Delta n/\left(\lambda \cos\Theta_s^{in}\right), \tag{8}$$

where Γ and Δn are the corresponding steady-state values for gain factor and light-induced refractive index change caused by the PR effect.

Thus, the gain factor Γ may be evaluated from the experimental data on $T_{\min}$ with following expression:

$$\Gamma = \left(1/l_{eff}\right)[\ln\{\left(1 - T_{\min}\right)/(T_{\min} \times m_0)\}]. \tag{9}$$

However, quantitative evaluation of Γ values from the Z-scan data on $T_{\min}$ requires to know the values of m_0 and l_{eff} that are impossible to determine only from OA Z-scan data, according to Eq. (6). Meanwhile, the experimental data obtained (Fig. 5, Table 1) show clearly that Γ is monotonously increasing with P_{in} (i.e., with I_0), in full accordance with Eq. (8) and the well-established dependence of Δn on I_0 [40]. Besides, Γ values at a given level of P_{in} depend on the dopant type and concentration (Fig. 4, Tables 1, 2).

The recent data [41] show that refractive index modulation is in good agreement with captured carriers' distribution and not with distribution of space-charge field performed by photovoltaic effect in lithium niobate crystals. It means that the refractive index modulation in PR LiNbO$_3$ is not caused only by macroscopic charges separation as it is supposed by standard model PR effect [27, 40], but it is caused by local changes of the polarization (dipole moment) of the traps when they capture an electron. The latter creates the field responsible for the dynamic-state PR effect, and it is due to the photoexcitation of defect-centered dipoles [41]. The photoexcited electrons are, indeed, still tied to the defect centers and relax back to the ground state when the light is turned off. Furthermore, the speckle pattern for output beam is changing in time ("self-pulsing" phenomenon [42]) as a result of the formation of dynamic gratings due to the dynamic-state PR effect. The local changes of polarization induce microscopic-scale inhomogeneities of the refractive index in LiNbO$_3$ causing the seed scattering for holographic amplification [41, 42].

As shown in the previous study [43], the average level of residual amplitude modulation (RAM) in electro-optic phase modulators and the fluctuations of RAM display a linear dependence on the maximum PR index change. Thus, our approach to apply the Z-scan data on evaluation

of NLS may be used to deduce a general behavior of RAM in electro-optic modulators utilizing the differently doped and/or processed $LiNbO_3$ crystals.

5 Summary

It has been established that the wide-angle polarization-isotropic PILS represents a dominating contribution to the NLS in $LiNbO_3$ crystals and gives the significant transmission modulation observed by the OA Z-scan technique. Therefore, the measurement of the third-order non-linear optical susceptibility of $LiNbO_3$ by the Z-scan method with cw-laser excitation is hindered by NLS, even when low intensities are used. It has been established that the OA Z-scan data reported previously for cw-excitation are related to the magnitudes of NLS, but not to the magnitudes of TPA in $LiNbO_3$ crystals. The modified OA Z-scan experimental technique is proposed to obtain quantitative information about NLS, and, hence, about PILS. NLS has a significant magnitude in the undoped, Mg-doped, and strongly Zr-doped ($[Zr] \geq 2$ mol%) $LiNbO_3$ crystals at moderate and high light intensities, but the NLS has a larger magnitude even at low intensities in the moderately Zr-doped $LiNbO_3$. Appearance of such a strong NLS (i.e., PILS) correlates with observation of the moving speckle pattern and self-pulsation of output signal at a moderate input power of the extraordinarily polarized cw-laser beams in the moderately Zr-doped $LiNbO_3$ crystals. The NLS is explained by holographic amplification of the seed scattering due to photorefractive effect. The gain factor for this amplification process is found to increase with the input power (i.e., with the light intensity).

References

1. Q. Wang Song, C.P. Zhang, P.J. Talbot, Self-defocusing, self-focusing, and speckle in LiNbO₃ and LiNbO₃Fe crystals. Appl. Opt. **32**, 7266–7271 (1993)
2. M. Sheik-Bahae, A.A. Said, T.-H. Wei, D.J. Hagan, E.W. Van Stryland, Sensitive measurement of optical nonlinearities using a single beam. IEEE J. Quantum Electron. **26**, 760–769 (1990)
3. R. DeSalvo, A. Said, D. Hagan, E. Van Stryland, M. Sheik-Bahae, Infrared to ultraviolet measurements of two-photon absorption and n₂ in wide bandgap solids. IEEE J. Quantum Electron. **32**, 1324–1333 (1996)
4. B. Gu, J. Wang, J. Chen, Y.-X. Fan, J. Ding, H.-T. Wang, Z-scan theory for material with two- and three-photon absorption. Opt. Express **13**, 9230–9234 (2005)
5. M. Rumi, J.W. Perry, Two-photon absorption: an overview of measurements and principles. Adv. Opt. Photonics **2**, 451–518 (2010)
6. R. de Nalda, R. del Coso, J. Requejo-Isidro, J. Olivares, A. Suarez-Garcia, J. Solis, C.N. Afonso, Limits to the determination of the nonlinear refractive index by the Z-scan method. J. Opt. Soc. Am. B **19**, 289–296 (2002)
7. S.M. Kostritskii, M. Aillerie, E. Kokanyan, Investigation of nonlinear refraction and absorption in Mg- and Zr-doped LiNbO₃ with the aid of Z-scan techniques. Proc. SPIE **9065**, 906508 (2013)
8. F.Z. Henari, K. Cazzini, F.E. Akkari, W.J. Blau, Beam waist changes in lithium niobate during Z-scan measurement. Appl. Phys. Lett. **78**, 1373–1375 (1995)
9. MdM Parvez, Experimental studies on the nonlinear optical properties of LiNbO₃ crystals. Am. J. Sci. Ind. Res. **6**, 69–73 (2015)
10. L. Palfalvi, J. Hebling, G. Almasi, A. Peter, K. Polgar, K. Lengyel, R. Szipcs, Nonlinear refraction and absorption of Mg doped stoichiometric and congruent LiNbO₃. J. Appl. Phys. **95**, 902–908 (2004)
11. Y. Chen, S.W. Liu, D. Wang, T. Chen, M. Xiao, Measurement of laser-induced refractive index change of inverted ferroelectric domain LiNbO₃. Appl. Opt. **46**, 7693–7696 (2007)
12. S.M. Kostritskii, M. Aillerie, Z-scan study of nonlinear absorption in reduced LiNbO₃ crystals. J. Appl. Phys. **111**, 103504 (2012)
13. S.M. Kostritskii, M. Aillerie, Optical damage in reduced Z-cut LiNbO₃ crystals caused by longitudinal photovoltaic and pyroelectric fields. J. Appl. Phys. **111**, 013519 (2012)
14. Q.Q. Wang, J. Shi, B.F. Yang, H.L. Liu, G.G. Xiong, Q.H. Gong, Q.K. Xue, A Z-scan study of LiNbO₃ thin film. Chin. Phys. Lett. **19**, 677–679 (2002)
15. N.Y. Kamber, G. Zhang, S. Liu, S.M. Mikha, W. Haidong, Study of the self-defocusing in LiNbO₃:Fe, Mg crystals. Opt. Commun. **184**, 475–483 (2000)
16. J. Wen, ChY Gao, H.T. Yu, M. Zhao, J.J. Shang, X.L. Li, Investigation on third-order nonlinear optical properties of undoped LiNbO₃ by modified Z-scan technique. Appl. Phys. B **123**, 85 (2017)
17. L. Palfalvi, K. Lengyel, A. Peter, J.A. Fulop, T. Reiter, J. Hebling, Theoretical and experimental development of the Z-scan method and its application for the characterization of LiNbO₃. Proc. SPIE **7501**, 75010F (2009)
18. N. Venkatram, R.S.S. Kumar, D.N. Rao, Nonlinear absorption and scattering properties of cadmium sulphide nanocrystals with its application as a potential optical limiter. J. Appl. Phys. **100**, 074309 (2006)
19. V. Joudrier, P. Bourdon, F. Hache, C. Flytzanis, Nonlinear light scattering in a two-component medium: optical limiting application. Appl. Phys. B **67**, 627 (1998)
20. Y. Kong, S. Liu, Y. Zhao, H. Liu, S. Chen, J. Xu, Highly optical damage resistant crystal: Zirconium-oxide doped lithium niobate. Appl. Phys. Lett. **91**, 081908 (2007)
21. V. Degiorgio, P. Minzioni, G. Nava, I. Cristiani, W. Yan, D. Grando, N. Argiolas, M. Bazzan, M.V. Ciampolillo, A.M. Zaltron, C. Sada, Photorefractivity of zirconium-doped lithium niobate. Proc. SPIE **8071**, 80710R (2011)
22. S. González-Martínez, J. Castillo-Torres, J.A. Hernández, H.S. Murrieta, J.G. Murillo, R. Farias, Experimental evidence of a non-relationship between photorefractive inhibition and photoconductivity increase in LiNbO₃:Mg. Opt. Commun. **282**, 1212–1219 (2009)

23. E. Kokanyan, E.J. Dieguez, New perspectives of lithium niobate crystals. Optoelectr. Adv. Mater. **2**, 205–214 (2000)

24. https://goochandhousego.com/wp-content/uploads/2013/12/PPLN_DS.pdf

25. https://goochandhousego.com/wp-content/uploads/2013/12/LNmatProperties.pdf

26. http://www.roditi.com/SingleCrystal/LiNbO3/Magnesium-Doped.html

27. J.-J. Liu, P.P. Banerjee, Q. Wang Song, Role of diffusive, photovoltaic, and thermal effects in beam fanning in LiNbO$_3$. J. Opt. Soc. Am. B **11**, 1688–1693 (1994)

28. M.R.R. Gesualdi, C. Jacinto, T. Catunda, M. Muramatsu, V. Pilla, Thermal lens spectrometry in pyroelectric lithium niobate crystals. Appl. Phys. B **93**, 879–883 (2008)

29. F. Lüdtke, N. Waasem, K. Buse, B. Sturman, Light-induced charge-transport in undoped LiNbO$_3$ crystals. Appl. Phys. B **105**, 35–50 (2011)

30. S.M. Kostritskii, O.G. Sevostyanov, Influence of defects on light-induced changes in refractive index of lithium niobate. Appl. Phys. B **65**, 527–533 (1997)

31. R. Ganeev, I. Kulagin, A. Ryasnyansky, R. Tugushev, T. Usmanov, Characterization of nonlinear optical parameters of KDP, LiNbO$_3$ and BBO crystals. Opt. Commun. **229**, 403–412 (2004)

32. H. Li, F. Zhou, X. Zhang, W. Ji, Picosecond Z-scan study of bound electronic Kerr effect in LiNbO$_3$ crystal associated with two-photon absorption. Appl. Phys. B **64**, 659–662 (1997)

33. R.K. Choubey, R. Trivedi, M. Das, P.K. Sen, P. Sen, S. Kar, K.S. Bartwal, R.A. Ganeev, Growth and study of nonlinear refraction and absorption in Mg doped LiNbO$_3$ single crystals. J. Crys. Growth **311**, 2597–2601 (2009)

34. H. Badorreck, S. Nolte, F. Freytag, P. Bäune, V. Dieckmann, M. Imlau, Scanning nonlinear absorption in lithium niobate over the time regime of small polaron formation. Opt. Mater. Express **5**, 2729–2741 (2015)

35. H. Qiao, J. Xu, Q. Wu, X. Yu, Q. Sun, X. Zhang, G. Zhang, T.R. Volk, An increase of photorefractive sensitivity in In:LiNbO$_3$ crystal. Opt. Mater. **23**, 269–272 (2003)

36. G. Zhang, Q. Li, P. Ho, S. Liu, Z. Wu, R.R. Alfano, Dependence of specklon size on laser beam size via photo-induced light scattering in LiNbO$_3$:Fe. Appl. Opt. **25**, 2955–2958 (1986)

37. M. Goulkov, M. Imlau, Th Woike, Photorefractive parameters of lithium niobate crystals from photoinduced light scattering. Phys. Rev. B **77**, 235110 (2008)

38. M.A. Ellabban, M. Fally, R.A. Rupp, T. Woike, M. Imlau, Holographic scattering and its applications, in *Recent Research Developments in Applied Physics*, vol. 4, ed. by S. Pandalai (Transworld Publishing, India, 2001), pp. 241–275

39. M. Imlau, Th. Woike, M. Fally, M. Ellaban, R. A. Rupp and M. Goulkov, Non-linear light scattering in polar oxides at the example of strontium-barium-niobate. in R. Wasser, U. Bottger, S. Tiedke (Editors) Proceedings of POLECER Conference, Chapter VII, 148 (2003)

40. O. Althoff, E. Kratzig, Strong light-induced refractive index changes in LiNbO$_3$. Proc. SPIE **1273**, 12–19 (1990)

41. I. Turek, N. Tarjányi, Opt. Express **15**, 10782 (2007)

42. L. Wan, Y. Yuan, G. Assanto, Switching and self-pulsing with dynamic holographic gratings in photorefractive waveguides. Opt. Commun. **74**, 361–364 (1990)

43. J. Sathian, E. Jaatinen, Reducing residual amplitude modulation in electro-optic phase modulators by erasing photorefractive scatter. Opt. Express **21**, 12309–12317 (2013)